In Vivo Adipogenesis in Rats Measured by Cell Kinetics in Adipocytes and Plastic-Adherent Stroma-Vascular Cells in Response to High-Fat Diet and Thiazolidinedione

Yourka D. Tchoukalova,[1] Mark Fitch,[2] Pamela M. Rogers,[1] Jeffrey D. Covington,[1] Tara M. Henagan,[1] Jianping Ye,[1] Marc K. Hellerstein,[2,3] and Eric Ravussin[1]

Impairment of adipogenesis contributes to the development of obesity-related insulin resistance. The current in vitro approaches for its assessment represent crude estimates of the adipogenic potential because of the disruption of the in vivo microenvironment. A novel assessment of in vivo adipogenesis using the incorporation of the stable isotope deuterium (^{2}H) into the DNA of isolated adipocytes and stroma-vascular fraction from adipose tissue has been developed. In the current study, we have refined this technique by purifying the adipocytes via a negative immune selection and sorting the plastic adherent stroma-vascular (aSV) subfraction (using 3 h culture) that contains mostly adipocyte progenitor cells and ~10% of small adipocytes. Using a 3-week 8% ^2H_2O ingestion with a high-fat diet (HFD) or HFD plus pioglitazone (HFD-P), we demonstrate that the fractions of new aSV cells (f_{aSV}) and immunopurified adipocytes (f_{AD}) (the ratio of their ^{2}H-enrichment of DNA to the maximal ^{2}H-enrichment of DNA of bone marrow reference cells) recapitulate the known hyperplastic mechanism of weight gain with pioglitazone treatment. We conclude that f_{aSV} and f_{AD} are reliable indices of in vivo adipogenesis. The proposed method represents a valuable tool for studying the effect of interventions (drugs, diets, and exercise) on in vivo adipogenesis. ***Diabetes*** **61:137–144, 2012**

Studies indicate that adipogenesis is an important mechanism in the prevention of adipocyte hypertrophy, upper-body fat distribution, and insulin resistance, all of which are associated with increased risk of the development of the metabolic syndrome (1–3). Adipogenesis involves commitment of stem cells to the adipocyte lineage, proliferation of stem cells and preadipocytes, recruitment of preadipocytes for differentiation to adipocytes (4), and terminal differentiation or maturation of adipocytes (5). Microenvironmental factors in the adipose tissue, including hormonal and oxygenation factors, innervation, and interactions with other cell types and the extracellular matrix, all influence adipogenesis (6–11). Current methods indirectly assess adipogenesis in adipose-derived stroma-vascular cultures (12) or by determining gene/protein expression of factors involved in adipogenesis regulatory pathways. These approaches represent crude estimates of the adipogenic process because of the disruption of in vivo microenvironmental influences. While these techniques are informative, methods providing an integrative evaluation of adipogenesis within the natural microenvironment would provide invaluable insight.

A method, based on the incorporation of deuterium (^{2}H) into covalent C-H bonds in the deoxyribose moiety of newly synthesized DNA of dividing cells, has been developed for assessment of cell proliferation in vivo (13,14). In short-term experiments, cells with slow turnover have not attained their maximal DNA ^{2}H-enrichement, whereas cells with rapid turnover (i.e., bone marrow and monocytes) replace their DNA quickly and reach a plateau, thus serving as an internal reference for the assay. The ratio of ^{2}H-enrichment of DNA from the cell of interest to that from reference cells indicates the fractional replacement of DNA or the fraction of newly divided cells of interest (f) (13). Two studies have been conducted with the use of this isotopic method for assessment of in vivo adipogenesis in stroma-vascular fractions and adipocytes (15,16). However, the interpretation of the results of these studies was hampered by the potential contamination of adipocytes and their progenitors with other cell types. Therefore, the main goal of this study was to optimize the method as follows: *1*) by purifying the adipocytes via a negative immune selection and *2*) by obtaining a stroma-vascular subfraction that is enriched in progenitor cells by exploiting their property to attach to plastic after a short-term culture of the stroma-vascular cells (17,18). The fractions of purified adipocytes (f_{AD}) and adherent stroma-vascular cells (f_{aSV}) were determined. A high-fat diet (HFD) and a HFD supplemented with pioglitazone (HFD-P) were used to demonstrate the effectiveness of this method, since thiazolidinediones are believed to amplify the hyperplastic mechanism of the HFD-induced fat accumulation (19).

RESEARCH DESIGN AND METHODS

Thirty-two 50- to 55-day-old male Long-Evans rats (Harlan Laboratories, Indianapolis, IN) were fed ad libitum rodent LabDiet (5% of calories from fat) and water for 1 week prior to the experiments. The rats were weighed twice a week during the following dietary and ^2H_2O-drinking interventions. All procedures were approved by the institutional animal care and use committee at the Pennington Center.

Diet intervention. The rats were divided into three groups and fed ad libitum the following diets (Research Diets, New Brunswick, NJ) for 21 days: *1*) low-fat diet (LFD) (10% of calories from fat, cat. no. D12450B), n = 10; *2*) HFD (60% of calories from fat, cat. no. D12492), n = 11; and 3) HFD-P containing 0.033% pioglitazone (providing 20 mg · kg^{-1} · day^{-1} given a daily consumption of 15 g of food), n = 11.

^2H_2O-labeling protocol. On the first day of the dietary intervention, all rats received an intraperitoneal bolus injection of 35 mL/kg body wt 0.9% NaCl in 100% ^2H_2O (Cambridge Isotope Laboratories, Andover, MA) after isoflurane anesthesia. Previous studies have shown that loading this dose achieves a 5% body-water enrichment (13). For maintenance of this level of ^2H_2O enrichment, rats were given ad libitum access to 8% ^2H_2O for the 21-day

From the [1]Pennington Biomedical Research Center, Louisiana State University System, Baton Rouge, Louisiana; the [2]Department of Nutrition and Toxicological Sciences, University of California, Berkeley, Berkeley, California; and the [3]Diabetes Center, University of California, San Francisco, San Francisco, California.
Corresponding author: Yourka D. Tchoukalova, yourka.tchoukalova@pbrc.edu.
Received 20 December 2010 and accepted 19 October 2011.
DOI: 10.2337/db10-1768

dietary intervention (13,14). Rats were killed, and epididymal adipose tissue (eAT) was collected. One part was snap-frozen in liquid N_2 for RNA extraction, and another was fixed in 4% paraformaldehyde, embedded in paraffin, and sectioned at 5 μm for immunohistochemistry. The remaining tissue was collagenase digested to isolate adipocytes and stroma-vascular cells as previously described (20).

Bone marrow cell isolation. The proximal ends of the removed femurs were clipped, placed in 2-mL vials supported by plastic inserts, and centrifuged for 5 s at 2,000 rpm as previously described (21,22). The extruded bone marrow cells were frozen in liquid N_2 and stored at −80°C.

Isolation of purified adipocytes and adherent stroma-vascular cells. The isolated adipocytes from LFD (n = 5), HFD (n = 6), and HFD-P (n = 6) rats were divided into two aliquots. One aliquot was frozen in liquid N_2 and stored at −80°C. The other aliquot was incubated with a cocktail of mouse monoclonal antibodies against markers of rat endothelial cells (CD31, cat. no. 1MCA1334G; AbD Serotec, Oxford, U.K.), nucleated hematopoietic cells (CD45, clone OX-1; Invitrogen, Camarillo, CA), and stem cells (nerve growth factor receptor p75NTP, i.e., CD271 [23], cat. no. MC192, Novus Biologicals, Littleton, CO] for 20 min at room temperature. Cells attached to the antibodies were discarded by using magnetic Dynabeads Pan Mouse IgG (Invitrogen, Camarillo, CA). The immunopurified adipocytes were frozen in liquid N_2 and stored at −80°C. The isolated adipocytes from the remaining animals were directly frozen in liquid N_2 and stored at −80°C until DNA extraction.

For isolation of an enriched population of adipocyte progenitor cells, a protocol for the isolation of mesenchymal stem cells from bone marrow cells using a short-term culture was used (24). The stroma-vascular fraction isolated from eAT was reconstituted in erythrocyte lysis buffer (0.154 mol/L NH_4Cl, 10 mmol/L $KHCO_3$, and 1 mmol/L EDTA) for 5 min at room temperature, centrifuged, reconstituted in 10% FBS in Dulbecco's modified Eagle's Medium/F-12 medium, and cultured for 3 h. The nonadherent cells were washed twice with PBS. The adherent stroma-vascular (aSV) cells were detached (0.25% trypsin/EDTA) and centrifuged, and the pellet was frozen in liquid N_2 and stored at −80°C.

DNA preparation and gas chromatography–mass spectrometry analysis. DNA from bone marrow cells was extracted by using a QiaAmp micro-DNA extraction kit (QIAGEN, Germantown, MD). DNA from the adipocytes and the aSV cells was extracted following the protocol for samples with a low number of cells (13). DNA was enzymatically hydrolyzed to free deoxynucleosides, and their deoxyribose moiety was converted to the tetrafluorobenzylpentosetriacetate derivative (13). Enrichment analysis of three replicates was performed on an Agilent 6890/5973 GC/MS equipped with a 30-m DB-17 column (250 μm inner diameter, 25-μm film thickness) using methane NCI and collecting ions in selected ion-monitoring mode at mass-to-charge ratios 435 and 436 (13). Unenriched DNA standards were used to correct for abundance sensitivity, and enrichment of the M+1 ion above natural abundance values were used to calculate the f_{AD} and f_{aSV}.

Immunocytochemistry. The aSV cells isolated from the eAT of three additional male Long-Evans rats on rodent LabDiet (5% of calories from fat) and at a weight (~400 g) comparable with that of the experimental rats were cytospun as previously described (25). The cytospun cells were incubated overnight (4°C) with primary antibodies (at 1:100) against mouse adipocyte protein (aP)2 (equivalent to human fatty acid–binding protein 4) (Dr. D. Bernlohr, Department of Biochemistry, Molecular Biology and Biophysics, University of Minnesota, Minneapolis, MN), rat CD34 (cat. no. AF4117; R&D Systems), rat CD31 (cat. no. 550300; BD Pharmingen, San Diego, CA), and rat CD11b/c (cat. no. MCA275EL, clone OX-42; AbD Serotec, Oxford, U.K.)] followed by 20-min incubations (at room temperature) with species-relevant fluorescently labeled secondary antibodies. The nuclei were stained with DAPI. Images were obtained on a confocal microscope (Leica SP5) at 200× magnification. The percentages of adipocyte progenitors ($CD34^+CD31^-$ cells), small immature adipocytes ($aP2^+$ cells), endothelial cells ($CD34^+CD31^+$ cells), and monocytes/macrophages ($CD11b/c^+$ cells) were determined.

Adipocyte size. Digital images from hematoxylin-eosin–stained sections were collected using a Zeiss Axioskope microscope (Carl Zeiss, Goettingen, Germany). The adipocyte area was measured in 4–5 fields using ImageJ software (http://rsbweb.nih.gov/ij/).

Immunohistochemistry and immunostaining. Sections were incubated overnight (4°C) with primary antibodies against the lipid droplet-associated protein perilipin (at 1:200, cat. no. ab3526; Abcam, Cambridge, MA) or the macrophage marker CD11b/c (at 1:100, clone OX-42; AbD Serotec), followed by an incubation with a fluorescein isothiocyanate–conjugated secondary antibody (at 1:400, cat. no. F2765; Invitrogen, Carlsbad, CA). Transferase-mediated dUTP nick-end labeling (TUNEL) staining was performed the following day per the manufacturer's protocol (cat. no. 12156792910; Roche Applied Science, Indianapolis, IN). Images were captured using a Zeiss Axioplan 2 upright microscope and Slidebook software, version 2.0 (both from Intelligent Imaging Innovations, Denver, CO). Two to five different areas within one to three sections from 7–10 different animals for each treatment group were analyzed using ImageJ.

In vitro proliferation of aSV cultures. The assay was performed to understand whether in vitro proliferation of cultured aSV cells reflects f_{aSV}. The stroma-vascular cells were seeded at a density of 0.5×10^4 cells/cm^2 in triplicate in 20% FBS in Dulbecco's modified Eagle's medium/F-12 medium. After 1, 4, 6, and 8 days, the nuclear content of the cultures was determined using a CyQuant NF Cell Proliferation Assay kit (Invitrogen) and converted to cell number using a standard curve with a known number of cells. The number of cell doublings at each time point was determined according to the following formula: CD = ln(Nf:Ni)/ln2, where CD is cell doublings, Nf is final number of cells, and Ni is initial (day 1) number of cells (26). The doubling time was calculated by dividing the culture time by cell doublings (26).

Quantitative real-time PCR for markers of adipose cell differentiation. RNA from the eAT of eight animals per group was extracted with TRIzol (Invitrogen) and an RNeasy kit (QIAGEN, Valencia, CA). The yield and purity of RNA were determined using the Nanodrop ND1000 Spectrophotometer (Agilent Technologies, Palo Alto, CA). One microgram of RNA was treated with DNase I (Life Technologies, Carlsbad, CA) and reverse transcribed to cDNA (High Capacity cDNA Reverse Transcription kit; Applied Biosystems, Foster City, CA). The gene expression of inhibitors (Wnt 10b [27] and Pref-1 [28,29)]) and stimulators (peroxisome proliferator–activated receptor [PPAR]γ, its upstream transcriptional inducer zfp423 [30)] and its target aP2) of adipocyte differentiation was determined by RT-PCR (Table 1). The measurements were performed in triplicate on an ABI PRISM 7900 (Applied Biosystems, Branchburg, NJ) sequence detection system. Glyceraldehyde-3-phosphate dehydrogenase (*GAPDH*) expression was used for data normalization. The ΔC_T values (C_T value of each sample minus C_T value of *GAPDH*), the $\Delta\Delta C_T$ values (ΔC_T for each gene minus the mean ΔC_T of the same gene in LFD rats [control]), and the fold changes relative to the control ($2^{-\Delta\Delta CT}$) were calculated.

Statistical analysis. One- or two-way ANOVA followed by post hoc Tukey tests was performed using SAS statistical software (version 9.1.3; SAS, Cary, NC) to determine differences among the groups with α set at 0.05. Group differences in body weight were tested by repeated-measures ANOVA with baseline weight as a covariate. Data are presented as means ± SE unless otherwise mentioned.

RESULTS

Weight. Rats on the HFD-P experienced immediate higher weight gain compared with rats on the LFD (P = 0.007 by day 4 [Fig. 1]), which remained higher thereafter. The HFD rats weighed more than LFD rats on day 10 (P = 0.03) and later. There was no statistical difference between the weights of HFD and HFD-P rats at any time during the dietary treatment.

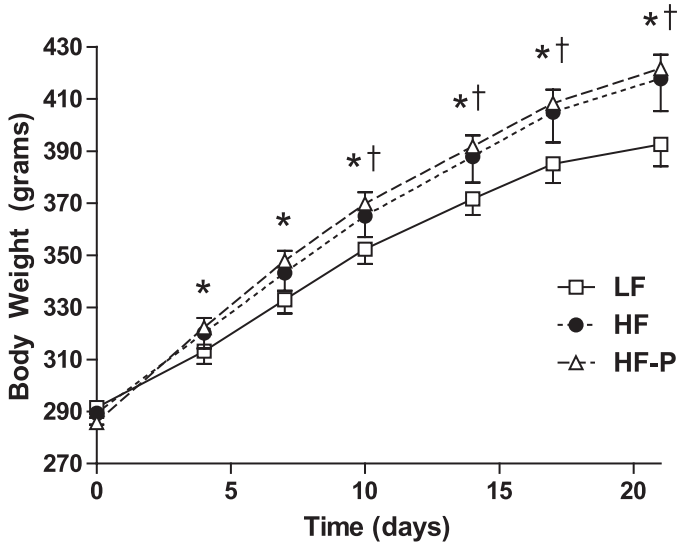

FIG. 1. Weights of rats along the course of 21 days of dietary treatment by group. Rats fed an LFD (LF) (10% of calories from fat; n = 10), an HFD (HF) (60% of calories from fat; n = 11), or an HFD-P (HF-P) (20 mg · kg^{-1} · day^{-1}; n = 11) were weighed every 3 or 4 days for 21 days. The weights (means ± SE) are plotted as a function of time. *Differences between HFD-P and LFD groups. †Differences between HFD and LFD groups.

Fractions of new adipocyte progenitors and adipocytes. The f_{aSV} in HFD-P rats was significantly higher than in the LFD and HFD groups (Fig. 2*A*). The difference in the f_{aSV} between HFD and LFD rats was of borderline statistical significance ($P = 0.058$). The f_{AD} was lower (~50%) than the f_{aSV} in all groups (Fig. 2*A* vs. *B–D*). Paired comparison of f_{AD} (nonpurified) and f_{AD} (immunopurified) from 11 animals from all diet groups was 42.9 ± 2.2 vs. 35.5 ± 1.1%, respectively; $P = 0.004$ (Fig. 2*B*), representing a 17% reduction in the fractional replacement value. The f_{AD} (nonpurified) in the HFD-P rats was significantly greater than that in the LFD group (50 ± 3 vs. 37 ± 3%; $P = 0.01$), whereas the f_{AD} (nonpurified) in the HFD rats (46 ± 3%) was not statistically different from that in either the HFD-P or the LFD group (Fig. 2*C*). In contrast, the f_{AD} (immunopurified) in HFD-P rats was greater than that in the HFD group (39 ± 1 vs. 33 ± 1%; $P = 0.04$), and the f_{AD} in the LFD group (46 ± 3%) was not different from either HFD-fed group (Fig. 2*D*).

Immunocytochemistry. The predominant (~70%) subfraction in the stroma-vascular cells was adipocyte progenitors, $CD34^+CD31^-$ cells (Fig. 3*A*). Importantly, ~10% of the remaining $CD34^-$ aSV cells were $aP2^+$ cells, demonstrating a separate population of small adipocytes (Fig. 3*B*). Collectively, ~80% of the aSV cells are involved in adipogenesis. There were small contaminations with endothelial cells (0.5%, $CD34^+CD31^+$ cells) and macrophages (3.3%, $CD11b/c^+$ cells). Approximately 16.2% of the cells were not characterized.

In vitro proliferation of stroma-vascular cultures. The number of cell doublings of stroma-vascular cultures was not different among the groups and time points. For all time points combined, the number of cell doublings in LFD, HFD, and HFD-P rats were 1.0 ± 0.1, 1.1 ± 0.1, and 0.8 ± 0.1, respectively. The doubling time was also not different among the groups but increased significantly from day 3 to day 5 or day 7 ($P = 0.02$ and $P = 0.0002$, respectively), indicating increased contact inhibition. For

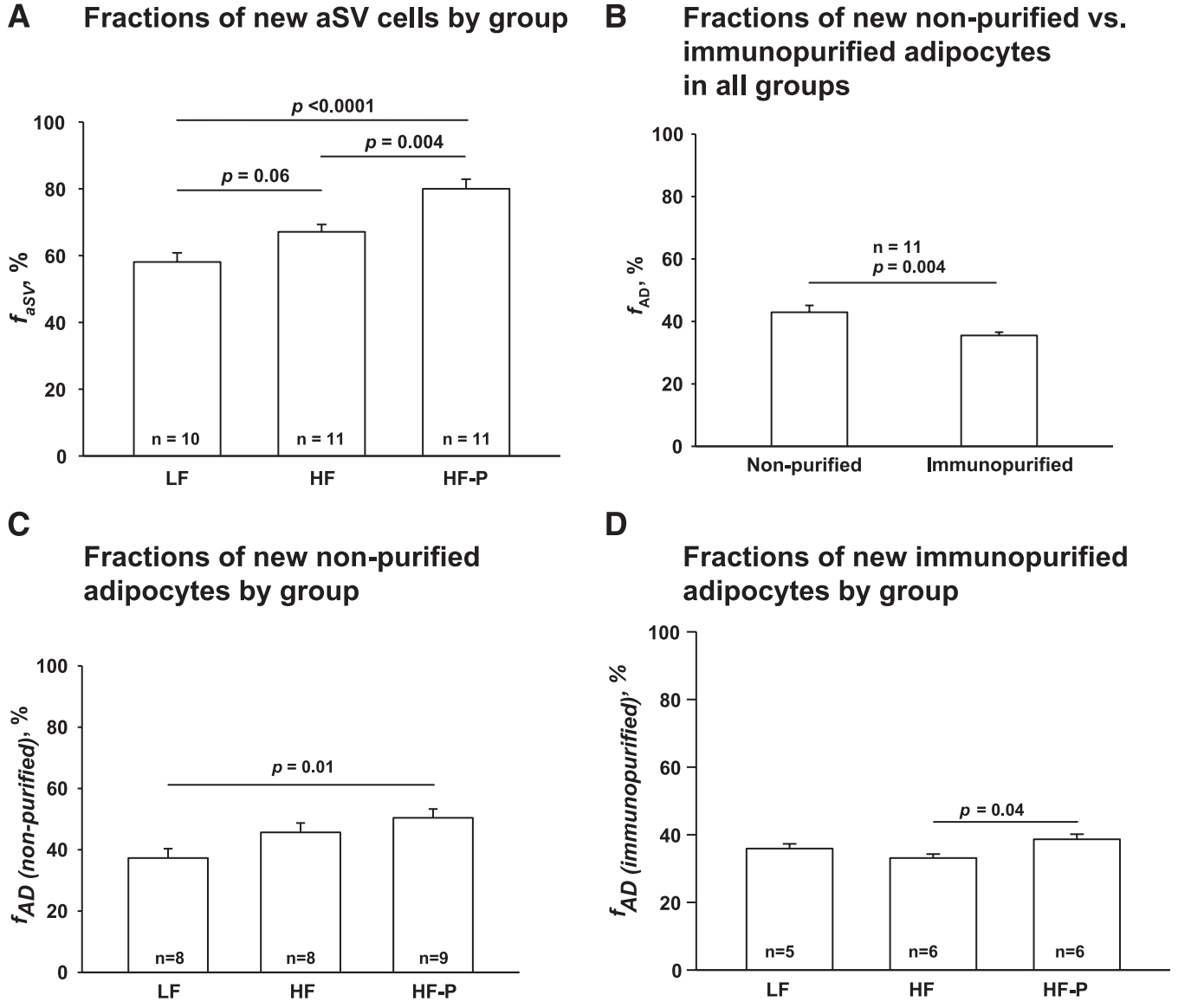

FIG. 2. Indices of in vivo adipogenesis. *A*: f_{aSV}. *B*: f_{AD} (nonpurified) vs. f_{AD} (immunopurified) (paired comparison) when all diets are combined. *C*: f_{AD} (nonpurified). *D*: f_{AD} (immunopurified). The fractions of aSV cells and adipocytes were relative to bone marrow cells in rats fed an LFD, an HFD, or an HFD-P, and were determined after 21-day labeling with 8% ^2H_2O. Values are group means ± SEs.

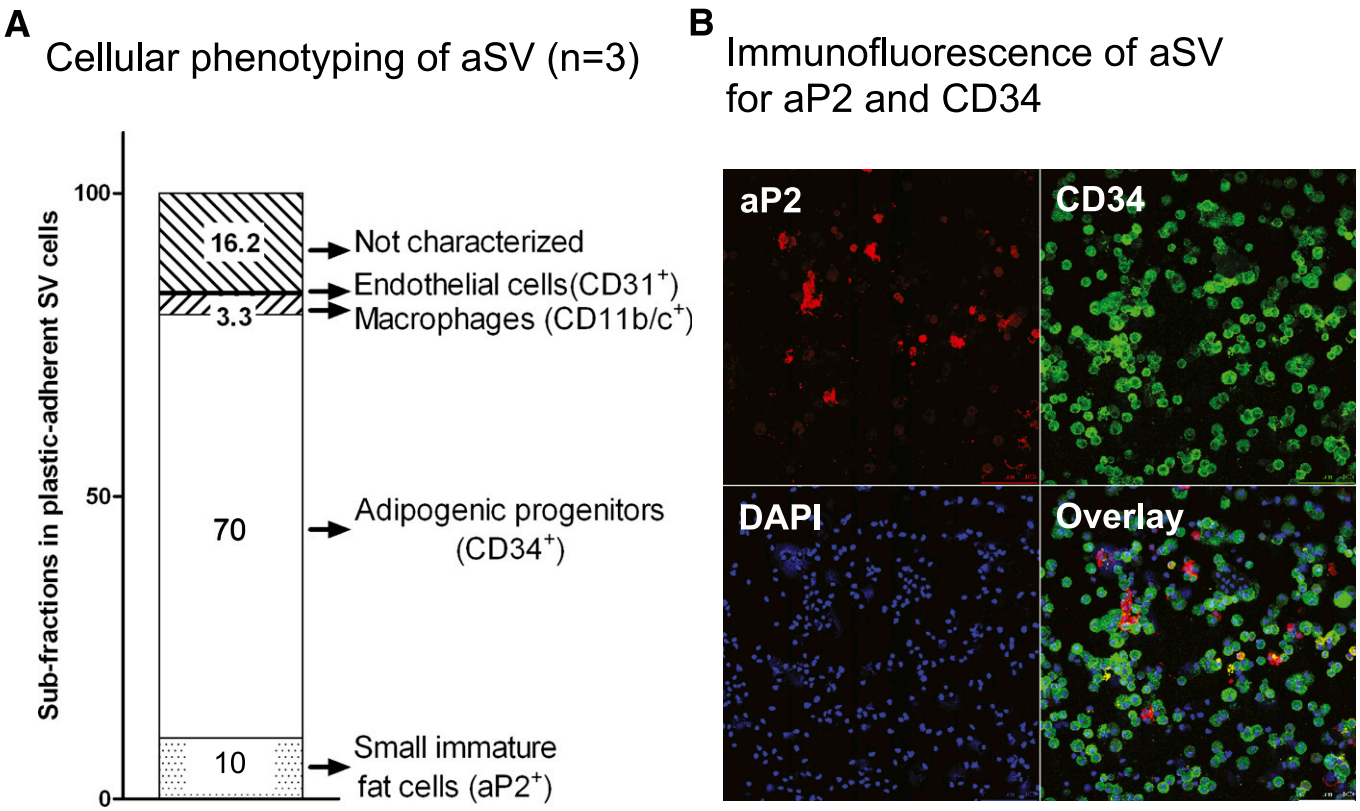

FIG. 3. Characterization of the aSV cells. *A*: The fractions of the individual subpopulations in plastic aSV cells from three rats fed ad libitum rodent LabDiet (5% of calories from fat) (in percent). *B*: Immunofluorescence of cytospun aSV cells identifying adipocytes, aP2$^+$ cells, and adipocyte progenitors, CD34$^+$CD31$^-$ cells. (A high-quality digital representation of this figure is available in the online issue.)

all groups, the doubling time at days 3, 5, and 7 of culture was 4.3 ± 0.7, 7.1 ± 0.7, and 8.7 ± 0.8 days, respectively.

Fat cell size, apoptosis, and adipose tissue fibrosis. The adipocyte size (surface area) was comparable (P = 0.2) among the groups: LFD, 3,046 ± 281 μm^2; HFD, 3,684 ± 268 μm^2; and HFD-P, 3,253 ± 281 μm^2. For further characterization of the adipocytes of the LFD and HFD groups, cell death was assessed in eAT from all groups. HFD-P adipose tissue exhibited the largest amount of cell death, as evidenced by the higher TUNEL staining in the HFD-P group (282.5 ± 34.5) compared with both the LFD (183.8 ± 20.0) and HFD (146.7 ± 13.1) groups (P = 0.0002 [Fig. 4*A* and *B*]). There was no statistical difference in overall cell death between the LFD and HFD groups (Fig. 4*B*). For further characterization of cell death, TUNEL staining was performed in conjunction with staining for a macrophage marker (CD11b/c) and an adipocyte cell viability indicator (perilipin). As indicated by CD11b/c staining, HFD adipose tissue exhibited a significant increase in macrophage infiltration compared with that in both LFD and HFD-P groups ($P < 0.0001$), with LFD adipose tissue containing 33.1 ± 3.3% macrophages, HFD 51.1 ± 2.4%, and HFD-P 39.0 ± 2.8% (Fig. 4*C*). There was no difference in percentage of macrophages between the LFD and HFD-P groups (Fig. 4*C*). In addition, there was no difference in the percentage of macrophages contributing to overall counts of cell death in the adipose tissue (data not shown). However, of the macrophages present in the adipose tissue, both HFD (86.3 ± 2.2%) and HFD-P (80.7 ± 2.3%) groups showed an increase in the percentage of apoptotic macrophages, determined by dual CD11b/c and TUNEL-positive stained macrophages, compared with the LFD group (68.2 ± 4.2%; P = 0.0003 [Fig. 4*D*]). Regarding the adipocyte apoptosis, the perilipin intensity in the HFD-P group (22,184 ± 1,812 arbitrary units [AU]) was significantly higher compared with that in the HFD group (14,937 ± 1,578 AU; P = 0.033) but not the LFD group (16,636 ± 2,961 AU) (Fig. 5*A* and *B*). There was no difference in perilipin between the LFD and HFD groups (Fig. 5*B*) Thus, HFD-P treatment may have an anti-inflammatory effect by decreasing macrophage infiltration in response to HFD feeding, as well as increasing macrophage apoptosis in adipose tissue and sparing or improving adipocyte health by preventing adipocyte apoptosis.

Gene expression. The level of *PPARγ2* mRNA in HFD-P rats was significantly lower than that in LFD and HFD groups (Table 1), indicating a ligand-receptor negative feedback relationship. The level of *aP2* mRNA in rats in both HFD dietary groups was significantly higher than in the LFD rats. The expression of the remaining genes analyzed was similar among the groups.

DISCUSSION

The main goal of the current study was to refine the method previously described for the measurement of in vivo adipogenesis (13,14). Several potential improvements to this technique were tested in the context of high-fat feeding in the presence or absence of pioglitazone.

First, the stroma-vascular fraction was enriched in adipocyte progenitor cells by short-term culturing of isolated stroma-vascular cells to allow efficient and preferential attachment of cells from nonhematopoietic lineages to plastic (aSV) (24). Phenotyping of the aSV cells in rats fed

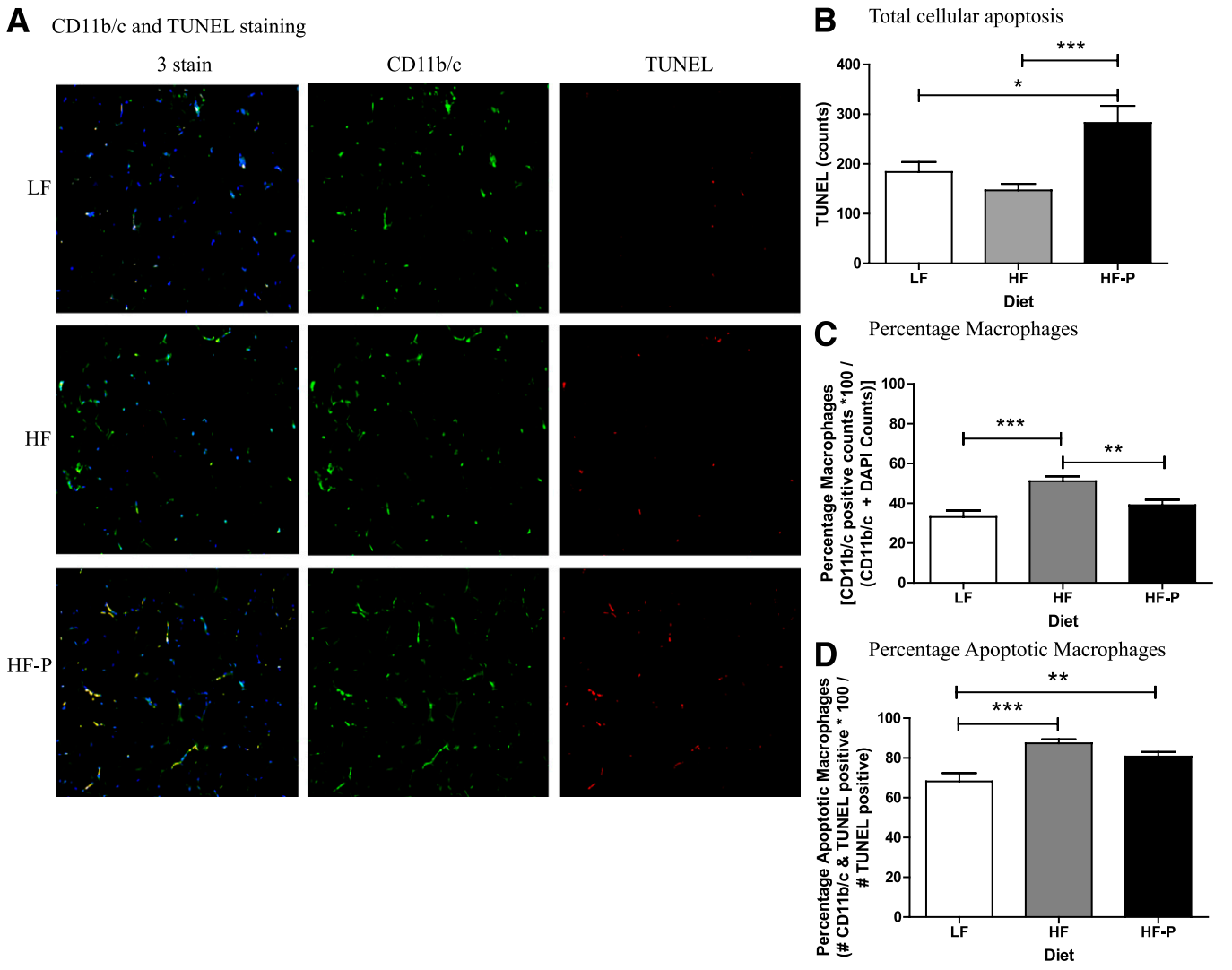

FIG. 4. Macrophage apoptosis in adipose tissue. *A*: TUNEL and CD11b/c staining. *B*: Apoptosis quantification. *C*: Macrophage quantification. *D*: Apoptotic macrophage quantification. **P* <0.05; ***P* <0.01; ****P* <0.0001. (A high-quality digital representation of this figure is available in the online issue.)

rodent LabDiet (5% of calories from fat) showed that 70% of aSV cells are adipogenic progenitor ($CD34^+CD31^-$) cells (31). We did not measure the percentage of $CD34^+CD31^-$ in the stroma-vascular fraction from the experimental rats. However, the noticeable reduction of the proportion of macrophages, from 33.1% $CD11b/c^+$ cells in adipose tissue of LFD-fed rats to 3.8% in the aSV cells, and the detection of a very small percentage of endothelial cells in aSV cells attest that an enrichment of aSV cells with adipocyte progenitors was achieved. Remarkably, an additional 10% of the aSV cells are $aP2^+$ cells. These cells are $CD34^-$ cells, indicating that they represent an independent subfraction from the adipocyte progenitor pool. We previously found $aP2^+CD68^-$ cells in human stroma-vascular fractions (25). We have also demonstrated that these cells may contain multiple small (<10 μm in diameter) lipid droplets, confirming that they are early differentiated (immature) adipocytes (25). Thus, we believe that the f_{aSV} reflects a component of early differentiation of adipocytes in addition to proliferation of adipocyte progenitor cells and possibly recruitment of preadipocytes to the adipocyte lineage, whereas the f_{AD} primarily indicates the terminal phase of differentiation.

However, a limitation to measuring the f_{AD} as an index of terminal differentiation is that other cell types with fast cell turnover, including hematopoietic, endothelial, and stem cells, may adhere to the floating adipocytes. In rodents, the probability for contamination, particularly with macrophages, is high owing to the considerable accumulation in the eAT (up to 50%) by high-fat feeding in our rats and in mice from other studies (32). Accordingly, a second potential improvement that we tested was to perform negative immune selection of the freshly isolated adipocytes and eliminate possible contamination with other cellular types. Importantly, the immunopurification step led to a significant reduction of the ^2H-content in DNA (to 83% of the values observed in nonpurified adipocytes). This reduction was larger in the HFD-fed rats that, interestingly, had the largest macrophage infiltration as evidenced by immunohistochemistry (CD11b/c). Together, our results suggest that contamination of adipocytes with other cell types may have contributed to an overestimation of the f_{AD} when measured without purification. Moreover, the immunopurification step led to differences between the group profiles of the f_{AD} (purified) versus f_{AD} (nonpurified) adipocytes, suggesting that the immunopurification of adipocytes

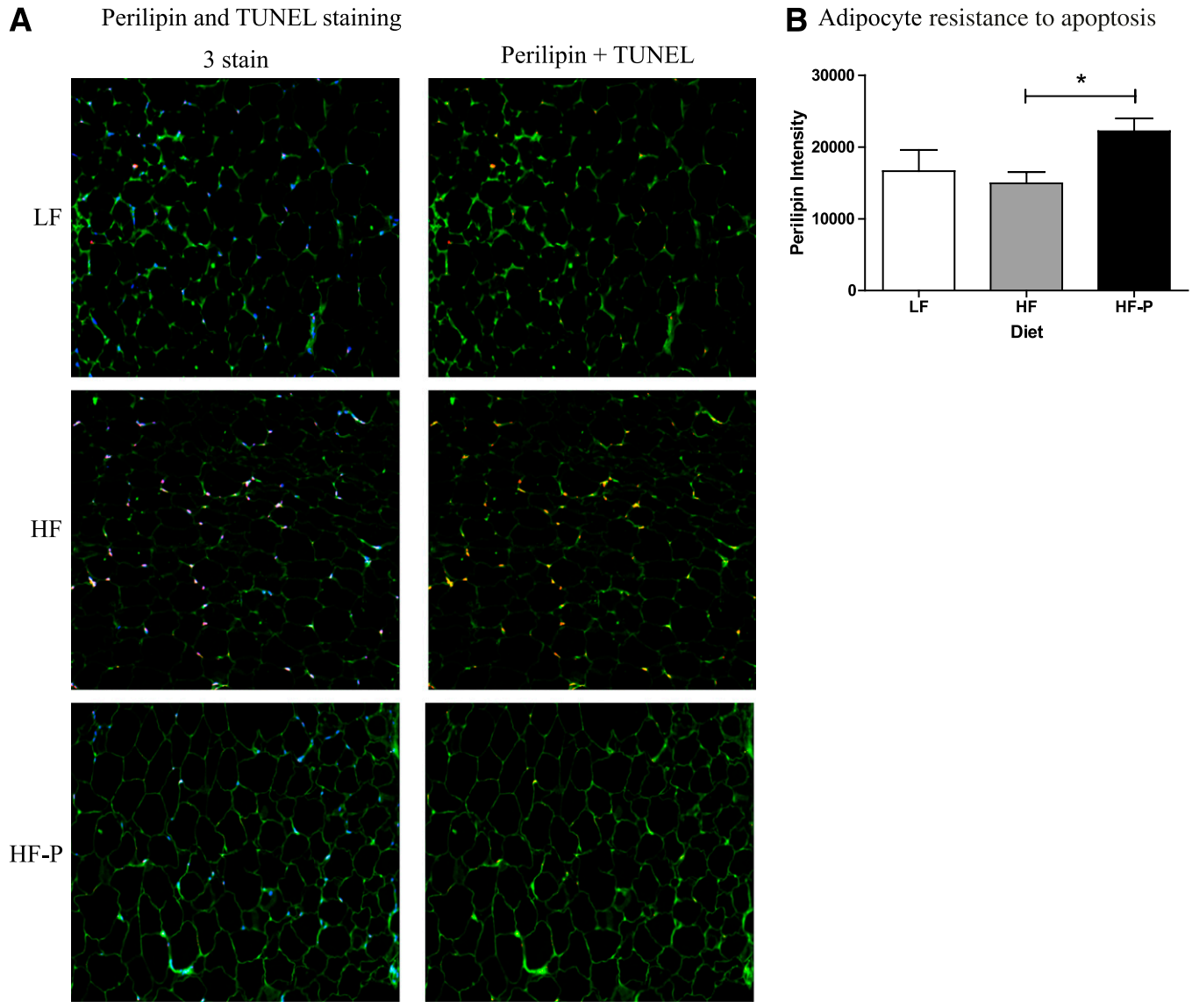

FIG. 5. Adipocyte apoptosis. *A*: Perilipin and TUNEL staining. *B*: Perilipin quantification. *P <0.05. (A high-quality digital representation of this figure is available in the online issue.)

may be beneficial. Finally, in line with previous findings (15), we show that the value of f_{aSV} is higher than that of f_{AD}. This potential for higher incorporation of ^2H into the DNA of aSV cells compared with adipocytes may allow for its more accurate determination.

The second aim of the study was to understand the relative importance of determining f_{aSV} and f_{AD} in reflecting induced adipogenesis. To test this, we included groups of rats fed an HFD in the presence or absence of pioglitazone. Pioglitazone is a member of the thiazolidinedione class

TABLE 1
Relative quantitation of the gene expression of regulators of adipogenesis in rat epididymal adipose tissue by treatment group

Gene	Taqman prime/probe sets*	Groups (n = 8 per group)			P
		LFD	HFD	HFD-P	
Pref 1	Rn01637113_g1	1.00 (0.5–1.9)	1.15 (0.8–1.6)	0.82 (0.3–2.0)	0.9
Wnt10b	Rn01532988_m1	1.00 (0.5–1.9)	1.57 (1.1–2.2)	0.83 (0.3–2.0)	0.06
PPARγ1	Rn00440945_m1	1.00 (0.5–1.9)[a]	1.06 (0.8–1.5)[ab]	0.57 (0.2–1.4)[b]	0.03
PPARγ2	Rn01492273_m1	1.00 (0.5–1.9)[a]	0.98 (0.7–1.4)[ab]	0.48 (0.2–1.2)[b]	0.02
aP2	Rn00670361_m1	1.00 (0.5–1.9)[a]	1.51 (1.1–2.1)[b]	1.43 (0.6–3.5)[b]	0.04
Zfp423	Rn00585834_ml	1.00 (0.5–1.9)	1.7 (1.2–2.4)	3.13 (1.3–7.6)	0.08

Data are the mean (range) fold difference compared with the mean expression in the control (LFD) group after normalization for the amount of GAPDH mRNA (probe Rn01749022_g1). *Pref 1*, preadipocyte factor 1; *Wnt10b*, wingless/Int-1; *Zfp423*, zinc finger protein 423. *Applied Biosystems (Foster City, CA). [a,b,ab]Different superscripts denote significant differences among the groups.

of drugs and a ligand for the key adipogenic transcription factor PPARγ. Studies suggest that it may contribute to the adipocyte hyperplastic mechanism of adipose tissue expansion in the context of energy excess (19,33–35). Interestingly, we found higher f_{aSV} in the HFD-P group versus the HFD alone and LFD groups but comparable f_{AD} between the HFD-P and LFD groups. These results are in line with previously reported data showing that 16-day treatment of obese Zucker rats with pioglitazone results in the appearance of new adipocytes and increased fat mass, but this is not coupled with a significant increase in newly formed adipocytes as assessed by the ^2H_2O incorporation in vivo (36). One possible mechanism explaining the increased f_{aSV} by pioglitazone is suggested by the increased *aP2* gene expression, increased perilipin protein expression, and decreased levels of *PPARγ* mRNA in the HFD-P vs. LFD rats, indicating potential formation of new, small, and metabolically active adipocytes. That these newly formed small adipocytes remain in the stroma-vascular fractions after centrifugation is also likely, as evidenced by the presence of very small lipid-containing $aP2^+CD68^-$ cells emitting strong fluorescent signal in the stroma-vascular fraction in our previous studies (25,37), as well as in the f_{aSV} in this study. One limitation of the current study is that the weight of the eAT depot was not determined, precluding an analysis of the relationship between f_{aSV} or f_{AD} and the number of adipocytes. However, other studies have shown that HFD-induced weight gain is due to increased total body fat (38) and increased eAT mass (19). Another limitation of our study is that the dynamics of the proportion of small to large adipocytes was not determined.

Compared with results in LFD rats, the HFD in the absence of pioglitazone led to a more gradual increase in the additional weight gain that was accompanied by a borderline increase in f_{aSV} along with no change in f_{AD} in HFD-fed rats. This suggests stimulation of clonal expansion and early phases of differentiation as possible mechanisms. We believe that the higher gene expression of *aP2* in the face of stable *PPARγ* in the HFD versus LFD group reflects this possibility through a mechanism of a direct stimulatory effect of fatty acids on aP2 transcription, independent of the induction of PPARγ transcriptional activity (39), along with a positive feedback loop in which aP2 facilitates the trafficking of fatty acids and their metabolites serving as ligands of PPARγ (40). Interestingly, a longitudinal monitoring of the recruitment of new inguinal adipocytes in growing genetically obese Zucker rats reveals a periodic wave of growth of inguinal adipose depot approximately every 55 days, starting with hyperplasia followed by hypertrophy (41). Strissel et al. (42) also demonstrated such waves of hyperplasia-hypertrophy-apoptosis in mice fed an HFD (60% of calories from fat) that were more prominent in the eAT compared with the inguinal depot and had a span of 20 weeks. The adipocyte hypertrophy was evident after 8 weeks of HFD feeding, explaining why it was not observed after the 3 weeks of HFD feeding in our study. Moreover, we generated evidence that apoptosis of hypertrophic adipocytes or restriction through extracellular fibrosis (data not shown) had not changed and thus had not inhibited the adipocyte enlargement. Taken together, these data support the potential hyperplastic mechanism of early phases of fat expansion induced by high-fat feeding. The supplementation of high-fat feeding with pioglitazone enhances both early phases of adipogenesis and terminal differentiation, as the f_{AD} in the HFD-P rats was significantly higher than in HFD rats. The observed anti-inflammatory effect of the pioglitazone through increased apoptosis of macrophages may be responsible, as it has been demonstrated that the macrophage recruitment and chronic inflammation in adipose tissue has been associated with impairment of adipocyte differentiation (43–45). Thus, our findings of similar weight gain but greater f_{aSV} and f_{AD} in the HFD-P vs. HFD group illustrate that measurement of f_{aSV} and f_{AD} facilitates the detection of small differences in the processes associated with in vivo adipogenesis. Interestingly, studies in C57BL/6 mice (C. Loe, M. Hellerstein, unpublished data) using the original technique showed increased f_{AD} and f_{aSV} with high-fat feeding, which were not further enhanced by adding pioglitazone. Differences in the methods and species may contribute to the disparities in the results.

In conclusion, f_{aSV} alone could be a reliable index of in vivo overall adipogenesis, while f_{AD} reflects primarily the adipocyte maturation rates. The measurement of f_{aSV} may be technically more feasible and sensitive for providing information on the effect of drugs or diets on overall in vivo adipogenesis. Further studies are needed to validate the feasibility and usefulness of the method in humans.

ACKNOWLEDGMENTS

This work was supported by Nutrition Obesity Research Center (NORC) Grant 1P30 DK072476 (to E.R.), entitled "Nutritional Programming: Environmental and Molecular Interactions" and sponsored by the National Institute of Diabetes and Digestive and Kidney Diseases, and by the National Institutes of Health (DK060412 to E.R.). This work used the facilities of the Cell Biology and Bioimaging Core, which are supported in part by a Centers of Biomedical Research Excellence grant (NIH P20-RR021945) and NORC center grants from the National Institutes of Health. M.K.H. has ownership interest in KineMed, Inc. No other potential conflicts of interest relevant to this article were reported.

Y.D.T. planned the study design, performed the experiment, wrote the first draft of the manuscript, and is the guarantor of the study. M.F. provided guidance for the DNA extraction, performed the gas chromatography–mass spectrometry analysis, and provided editorial assistance. P.M.R. performed RT-PCR and provided editorial assistance. J.D.C. performed immunocytochemistry and provided editorial assistance. T.M.H. performed immunohistochemistry and immunostaining, analyzed those data, described those techniques, and provided editorial assistance. J.Y. contributed to discussion and provided editorial assistance. M.K.H. maintained quality assurance of the gas chromatography–mass spectrometry methods, reviewed data, contributed to discussion, and provided editorial assistance. E.R. reviewed the proposal, provided funding, contributed to discussions, provided guidance for the development of the manuscript, and provided editorial assistance.

Parts of this work were presented in abstract form at the Obesity Society 28th Annual Scientific Meeting, San Diego, California, 8–12 October 2010.

The authors thank Shantele Thomas (now at Sanford/Burnham Institute, Orlando, Florida) for technical help.

REFERENCES

1. Vague J. The degree of masculine differentiation of obesities: a factor determining predisposition to diabetes, atherosclerosis, gout, and uric calculous disease. Am J Clin Nutr 1956;4:20–34
2. Weyer C, Foley JE, Bogardus C, Tataranni PA, Pratley RE. Enlarged subcutaneous abdominal adipocyte size, but not obesity itself, predicts type II

diabetes independent of insulin resistance. Diabetologia 2000;43:1498–1506
3. Arner E, Westermark PO, Spalding KL, et al. Adipocyte turnover: relevance to human adipose tissue morphology. Diabetes 2010;59:105–109
4. Avram MM, Avram AS, James WD. Subcutaneous fat in normal and diseased states 3. Adipogenesis: from stem cell to fat cell. J Am Acad Dermatol 2007;56:472–492
5. Tchoukalova YD, Harteneck DA, Karwoski RA, Tarara J, Jensen MD. A quick, reliable, and automated method for fat cell sizing. J Lipid Res 2003;44:1795–1801
6. Lai N, Jayaraman A, Lee K. Enhanced proliferation of human umbilical vein endothelial cells and differentiation of 3T3-L1 adipocytes in coculture. Tissue Eng Part A 2009;15:1053–1061
7. Hutley LJ, Herington AC, Shurety W, et al. Human adipose tissue endothelial cells promote preadipocyte proliferation. Am J Physiol Endocrinol Metab 2001;281:E1037–E1044
8. Lacasa D, Taleb S, Keophiphath M, Miranville A, Clement K. Macrophage-secreted factors impair human adipogenesis: involvement of proinflammatory state in preadipocytes. Endocrinology 2007;148:868–877
9. Chavey C, Mari B, Monthouel MN, et al. Matrix metalloproteinases are differentially expressed in adipose tissue during obesity and modulate adipocyte differentiation. J Biol Chem 2003;278:11888–11896
10. Cousin B, Casteilla L, Lafontan M, et al. Local sympathetic denervation of white adipose tissue in rats induces preadipocyte proliferation without noticeable changes in metabolism. Endocrinology 1993;133:2255–2262
11. Ye J. Emerging role of adipose tissue hypoxia in obesity and insulin resistance. Int J Obes (Lond) 2009;33:54–66
12. Armani A, Mammi C, Marzolla V, et al. Cellular models for understanding adipogenesis, adipose dysfunction, and obesity. J Cell Biochem 2010;110:564–572
13. Busch R, Neese RA, Awada M, Hayes GM, Hellerstein MK. Measurement of cell proliferation by heavy water labeling. Nat Protoc 2007;2:3045–3057
14. Turner SM, Roy S, Sul HS, et al. Dissociation between adipose tissue fluxes and lipogenic gene expression in ob/ob mice. Am J Physiol Endocrinol Metab 2007;292:E1101–E1109
15. Strawford A, Antelo F, Christiansen M, Hellerstein MK. Adipose tissue triglyceride turnover, de novo lipogenesis, and cell proliferation in humans measured with 2H2O. Am J Physiol Endocrinol Metab 2004;286:E577–E588
16. Neese RA, Misell LM, Turner S, et al. Measurement in vivo of proliferation rates of slow turnover cells by 2H2O labeling of the deoxyribose moiety of DNA. Proc Natl Acad Sci USA 2002;99:15345–15350
17. Tchkonia T, Tchoukalova YD, Giorgadze N, et al. Abundance of two human preadipocyte subtypes with distinct capacities for replication, adipogenesis, and apoptosis varies among fat depots. Am J Physiol Endocrinol Metab 2005;288:E267–E277
18. Tchkonia T, Lenburg M, Thomou T, et al. Identification of depot-specific human fat cell progenitors through distinct expression profiles and developmental gene patterns. Am J Physiol Endocrinol Metab 2007;292:E298–E307
19. Okuno A, Tamemoto H, Tobe K, et al. Troglitazone increases the number of small adipocytes without the change of white adipose tissue mass in obese Zucker rats. J Clin Invest 1998;101:1354–1361
20. Tchoukalova YD, Koutsari C, Karpyak MV, Votruba SB, Wendland E, Jensen MD. Subcutaneous adipocyte size and body fat distribution. Am J Clin Nutr 2008;87:56–63
21. Dobson KR, Reading L, Haberey M, Marine X, Scutt A. Centrifugal isolation of bone marrow from bone: an improved method for the recovery and quantitation of bone marrow osteoprogenitor cells from rat tibiae and femurae. Calcif Tissue Int 1999;65:411–413
22. Peister A, Mellad JA, Larson BL, Hall BM, Gibson LF, Prockop DJ. Adult stem cells from bone marrow (MSCs) isolated from different strains of inbred mice vary in surface epitopes, rates of proliferation, and differentiation potential. Blood 2004;103:1662–1668
23. Yamamoto N, Akamatsu H, Hasegawa S, et al. Isolation of multipotent stem cells from mouse adipose tissue. J Dermatol Sci 2007;48:43–52
24. Soleimani M, Nadri S. A protocol for isolation and culture of mesenchymal stem cells from mouse bone marrow. Nat Protoc 2009;4:102–106
25. Tchoukalova YD, Sarr MG, Jensen MD. Measuring committed preadipocytes in human adipose tissue from severely obese patients by using adipocyte fatty acid binding protein. Am J Physiol Regul Integr Comp Physiol 2004;287:R1132–R1140
26. Rainaldi G, Pinto B, Piras A, Vatteroni L, Simi S, Citti L. Reduction of proliferative heterogeneity of CHEF18 Chinese hamster cell line during the progression toward tumorigenicity. In Vitro Cell Dev Biol 1991;27A:949–952
27. Longo KA, Wright WS, Kang S, et al. Wnt10b inhibits development of white and brown adipose tissues. J Biol Chem 2004;279:35503–35509
28. Wang Y, Zhao L, Smas C, Sul HS. Pref-1 interacts with fibronectin to inhibit adipocyte differentiation. Mol Cell Biol 2010;30:3480–3492
29. Sul HS. Minireview: Pref-1: role in adipogenesis and mesenchymal cell fate. Mol Endocrinol 2009;23:1717–1725
30. Gupta RK, Arany Z, Seale P, et al. Transcriptional control of preadipocyte determination by Zfp423. Nature 2010;464:619–623
31. Sengenès C, Lolmède K, Zakaroff-Girard A, Busse R, Bouloumié A. Preadipocytes in the human subcutaneous adipose tissue display distinct features from the adult mesenchymal and hematopoietic stem cells. J Cell Physiol 2005;205:114–122
32. Weisberg SP, McCann D, Desai M, Rosenbaum M, Leibel RL, Ferrante AW Jr. Obesity is associated with macrophage accumulation in adipose tissue. J Clin Invest 2003;112:1796–1808
33. Adams M, Montague CT, Prins JB, et al. Activators of peroxisome proliferator-activated receptor gamma have depot-specific effects on human preadipocyte differentiation. J Clin Invest 1997;100:3149–3153
34. Smith SHX, Baghian S, Needham A, McNeil M, Bogacka I, Bray GA. Pioglitazone changes the distribution of adipocyte size in type 2 diabetics. Adipocyte 2006;2:11–22
35. McLaughlin TM, Liu T, Yee G, et al. Pioglitazone increases the proportion of small cells in human abdominal subcutaneous adipose tissue. Obesity (Silver Spring) 2010;18:926–931
36. Hunt D, Chen X, Santos M, et al. Increased adipose cell turnover is associated with increased insulin sensitivity in fa/fa obese Zucker rat. Abstract presented at the 2004 Annual Scientific Meeting of the North American Association for the Study of Obesity, 14–18 November 2004, Caesar's Palace, Las Vegas, Nevada
37. Tchoukalova Y, Koutsari C, Jensen M. Committed subcutaneous preadipocytes are reduced in human obesity. Diabetologia 2007;50:151–157
38. Schemmel R, Mickelsen O, Tolgay Z. Dietary obesity in rats: influence of diet, weight, age, and sex on body composition. Am J Physiol 1969;216:373–379
39. Distel RJ, Robinson GS, Spiegelman BM. Fatty acid regulation of gene expression. Transcriptional and post-transcriptional mechanisms. J Biol Chem 1992;267:5937–5941
40. Bernlohr DA, Coe NR, LiCata VJ. Fatty acid trafficking in the adipocyte. Semin Cell Dev Biol 1999;10:43–49
41. MacKellar J, Cushman SW, Periwal V. Waves of adipose tissue growth in the genetically obese Zucker fatty rat. PLoS ONE 2010;5:e8197
42. Strissel KJ, Stancheva Z, Miyoshi H, et al. Adipocyte death, adipose tissue remodeling, and obesity complications. Diabetes 2007;56:2910–2918
43. Isakson P, Hammarstedt A, Gustafson B, Smith U. Impaired preadipocyte differentiation in human abdominal obesity: role of Wnt, tumor necrosis factor-alpha, and inflammation. Diabetes 2009;58:1550–1557
44. Gustafson B, Gogg S, Hedjazifar S, Jenndahl L, Hammarstedt A, Smith U. Inflammation and impaired adipogenesis in hypertrophic obesity in man. Am J Physiol Endocrinol Metab. 21 July 2009 [Epub ahead of print]
45. Yarmo MN, Landry A, Molgat AS, Gagnon A, Sorisky A. Macrophage-conditioned medium inhibits differentiation-induced Rb phosphorylation in 3T3-L1 preadipocytes. Exp Cell Res 2009;315:411–418